A NEW METHOD FOR CALCULATING TRANSIENT ELECTROMAGNETIC RESPONSES OF AC/DC POWER SYSTEM WITH EXTERNAL ELECTROMAGNETIC PULSE INTERFERENCE

X.-Y. Huo and Y.-Z. Lei

Department of Electrical Engineering
Beihang University
Beijing 100191, China

Abstract—In this paper, a new method for calculating transient electromagnetic responses of AC/DC power system with external electromagnetic pulse interference is proposed. An input-output model of three-phase bridge rectifier is presented for the transient calculation. In order to study the effect of the external electromagnetic pulse on the system, the field-to-line coupling model is introduced, and finite-difference time-domain method is adopted. Thus, the modeling method utilizes the analysis methods of the electric circuits and electromagnetic fields synthetically to deal with the coupled field-circuit problems. The model and algorithm are validated by comparing the calculation results with the experiment ones. Finally, the effects of some circuit parameters on transient responses are discussed. The method proposed in this paper lays the foundation for further researches on the transient electromagnetic performance of independent electrical power systems containing power electronics.

1. INTRODUCTION

The electrical power systems of airplanes and marines move forward in the all-electric direction. Owing to the need of effective conversion and utilization of electrical energy, there is a great deal of the power electronic equipments (e.g., rectifier, inverter, and DC/DC converter, etc.) in power systems. The electromagnetic fields related to external electromagnetic pulse (EMP), for instance, lightning electromagnetic pulse (LEMP), nuclear electromagnetic pulse (NEMP) and high power

---

Corresponding author: X.-Y. Huo (huoxiaoyun@asee.buaa.edu.cn).

microwave (HPMW), produce transient overvoltages and overcurrents in the systems through the transmission lines. Consequently, these voltages and currents sometimes exceed the immunity limits of power electronic equipments connected with the ends of the transmission line, which could cause the failures of critical equipments, or even endanger the system safety. Therefore, it is crucial to predict the transient electromagnetic responses of the power system for EMP defense.

The EM scattering theory is generally used for researches on EMP coupling to transmission line. In many practical cases, Taylor model [1], Agrawal model [2], and Rachidi model [3] are sufficient for the field-to-line coupling. These models describe the distributed circuit with partial differential equations. The transient responses of the power system with EMP interference have been presented in many papers. Based on the analysis of electromagnetic field produced by external EMP, the transient responses of the transmission line with resistive loads were calculated by FDTD [4, 5]. The loss effect of the line for lossless transmission line was studied by computing the current induced at the end of a simple transmission line excited by an incident electromagnetic field in [6]. Based on the study of distributed circuit parameter, the responses of a bent transmission line with Gaussian pulse excitation were obtained in [7]. In [8], the singularity expansion method (SEM) and RLC circuit theory were used to calculate the transient responses by building the transfer function of the system and finding the poles in the complex frequency plane, which was not suitable for the nonlinear circuits.

The methods of calculating the transient responses for EMP coupling to transmission line with linear loads were extended to nonlinear loads. Huang attempted to analyze the responses of multiconductor transmission lines with nonlinear terminations under the periodic pulse excitation by using the harmonic balance technique [9]. Tesche adopted the electromagnetic topology method to analyze the line with nonlinear ends [10]. A method for transient analysis of multiconductor transmission line with nonlinear ends excited by an electric dipole was presented in [11]. Xie et al. presented the experimental study and SPICE simulation of transmission lines with transient voltage suppressors excited by a fast rise-time electromagnetic pulse [12]. However, the researches on the transient responses of power systems that consist of the transmission line and power electronic equipments have been done rarely.

The electromagnetic transients program (EMTP) was utilized to calculate the transient responses of system with EMP interference [13, 14]. Since the Bergeron method was adopted in EMTP [15], the voltage responses and current responses at any location along the

transmission line were hard to obtain.

Focusing on the power system which contains a three-phase bridge rectifier, a two-wire transmission line and loads, this paper proposes a new time domain modeling approach for calculating the transient electromagnetic responses of each junction of the system and any position of the transmission line. Moreover, a novel input-output model of three-phase bridge rectifier suitable for transient analysis is established, and the simple expressions make the programming easier. Incorporating with distributed parameter model of transmission line in time domain, the boundary conditions in discretized mathematical model by FDTD between lumped parameter models and distributed parameter models are given. The model and algorithm are validated by the comparison of calculation and experiment results of lightning surge simulated experiment.

This paper is organized as following: In Section 2, the model of field-to-line coupling is described and a new input-output model of three-phase bridge rectifier is proposed. In Section 3, the algorithm of the transient responses is presented. Section 4 implements the experiment to validate the model and algorithm. Section 5 discusses the effects of some system parameters on transient responses. Conclusions are made in Section 6.

2. MATHEMATICAL MODEL OF AC/DC POWER SYSTEM WITH THE EXTERNAL EMP INTERFERENCE

Figure 1 shows a typical AC/DC power system of aircraft with external EMP interference which is illustrated by an incident plane wave, and the time dependence of the E-field is expressed by a simple amplitude double exponential function. The EMP coupling to the power system through the transmission line can give rise to overvoltages and overcurrents on the line, which causes electromagnetic interference to the whole power system. The two ends of the transmission line are denoted by Networks 1 and 2, respectively. Network 1 is AC/DC power system which converts three-phase AC into DC by three-phase bridge rectifier, and Network 2 is composed of arbitrary loads whose voltage-current characteristics are known. Distributed parameter model is used for transmission line, and lumped parameter model is used for Networks 1 and 2.

Figure 1 also shows the AC/DC power system in the O-xyz coordinate system. The lumped circuit Network 1 lies on the origin of coordinate system. The transmission line is a long straight conductor. The x-axis follows the direction of the length of the transmission line,
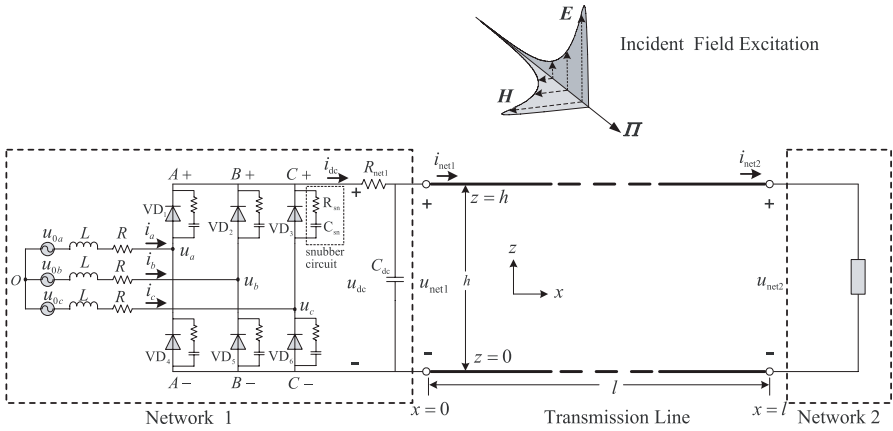
Figure 1. Diagram of an incident electromagnetic pulse interfering with AC/DC power system.

and z-axis follows the direction of the height of the transmission line. The line perpendicular to the xOz plane through the origin is the y-axis.

2.1. Time Domain Model of Field-to-line Coupling

In this part, the research focuses on two-wire parallel line with the external EMP interference, and the reflected fields from the ground or other shield objects are ignored. The time domain distributed parameter model of the field-to-line coupling should be utilized for analyzing the effects of EMP coupling on the power system. The transmission line equations in time domain introduced by Agrawal in [2] is adopted, which is expressed by scattered voltage $u^s(x,t)$ and line current $i(x,t)$ as

$$\begin{cases} \frac{\partial u^s(x,t)}{\partial x} + R_0 i(x,t) + L_0 \frac{\partial i(x,t)}{\partial t} = E_x^{\text{inc}}(x,0,h,t) - E_x^{\text{inc}}(x,0,0,t) \\ \frac{\partial i(x,t)}{\partial x} + G_0 u^s(x,t) + C_0 \frac{\partial u^s(x,t)}{\partial t} = 0 \end{cases} \quad (1)$$

where R_0, L_0, G_0, C_0 represent the per-unit-length parameters of the line, and E_x^{inc} is the component of electric field along the direction of x-axis. The total voltage $u(x,t)$ at any location along the line is the sum of scattered voltage $u^s(x,t)$ and incident voltage $u^i(x,t)$. Accordingly, the voltage boundary conditions of the two ends of the line are given by

$$u_{\text{net1}}(t) = u_1^i(t) + u_1^s(t) \quad (2)$$

$$u_{\text{net2}}(t) = u_{NDX+1}^i(t) + u_{NDX+1}^s(t) \quad (3)$$

where $u_{\mathrm{net1}}(t)$ and $u_{\mathrm{net2}}(t)$ are the total voltage at the ends of the transmission line with power supply and arbitrary load, respectively. $u_1^{\mathrm{i}}(t)$ and $u_1^{\mathrm{s}}(t)$ are incident voltage and scattered voltage at $x = 0$, respectively. Similarly, $u_{NDX+1}^{\mathrm{i}}(t)$ and $u_{NDX+1}^{\mathrm{s}}(t)$ are incident voltage and scattered voltage at $x = l$, respectively. The incident voltages of the two ends of the line are defined by

$$u_1^{\mathrm{i}}(t) = -\int_0^h E_z^{\mathrm{inc}}(0,0,z,t)\,\mathrm{d}z \tag{4}$$

$$u_{NDX+1}^{\mathrm{i}}(t) = -\int_0^h E_z^{\mathrm{inc}}(l,0,z,t)\,\mathrm{d}z \tag{5}$$

where E_z^{inc} is the component of electric field along z-axis caused by the EMP.

According to Eqs. (1)–(5), the effect of external EMP coupling to transmission line consists of two parts:

Part 1: distributed voltage sources along the line expressed by E_x^{inc} in Eq. (1) represent the effect of x-components of the incident electric field;

Part 2: lumped voltage sources at the ends of the line expressed by u_1^{i} and u_{NDX+1}^{i} in Eq. (2) and Eq. (3) represent the effect of z-components of the incident electric field.

2.2. Input-output Model of Three-phase Bridge Rectifier

The three-phase bridge rectifier is composed of six diodes. Mode means the different network composing loops by the six on/off status diodes, and the rectifier has the determinate mode at any moment.

An input-output model for three-phase bridge rectifier composed of high-power diodes is presented, which has uniform expressions and only needs to judge the on/off status of the diodes without considering the conditions of mode conversion of the rectifier.

The on/off status S_i of diodes VD_i (in Figure 1) is defined by

$$S_i = \begin{cases} 1, & \text{for } \mathrm{VD}_i \text{ switches on} \\ 0, & \text{for } \mathrm{VD}_i \text{ switches off} \end{cases} \tag{6}$$

where $i = 1, 2, \ldots, 6$ and the index of diodes is shown in Figure 1. When the high-power diode is used in low frequency rectifier, the dynamic process from the on status to the off status and the reverse process could be ignored. Therefore, it is assumed that the diode switches on when $S = 1$, and the diode switches on when $S = 0$ without any time delay in the proposed model.

If the ideal diode VD_i switches on, the model of VD_i is the critical voltage U_{d0i} in series with the resistance R_{dioi}. When the six diodes all switch on, the voltage matrix of diodes is expressed by

$$\mathbf{U}_{dio} = \mathbf{U}_{d0} + \mathbf{R}_{dio}\mathbf{I}_{dio} \tag{7}$$

where $\mathbf{U}_{dio} = [u_{dio1}, u_{dio2}, \ldots, u_{dio6}]^T$ is the voltage matrix of diodes; $\mathbf{I}_{dio} = [i_{dio1}, i_{dio2}, \ldots, i_{dio6}]^T$ is the current matrix through diodes; $\mathbf{U}_{d0} = [u_{d01}, u_{d02}, \ldots, u_{d06}]^T$ is the critical voltage matrix; and $\mathbf{R}_{dio} = \mathrm{diag}\{R_{dio1}, R_{dio2}, \ldots, R_{dio6}\}$ is the resistance matrix.

Each diode connects, in parallel, with a series $R_{sn} - C_{sn}$ snubber circuit, as shown in Figure 1. When the diodes switch off, the rectifier constitutes the loops through the snubber circuits. Consequently, $\mathbf{U}_{dio}$ can also be expressed by

$$\mathbf{U}_{dio} = \mathbf{U}_{C} + \mathbf{R}_{sn}\mathbf{I}_{sn} \tag{8}$$

where the voltage matrix of capacitances in the snubber circuits is $\mathbf{U}_{C} = [u_{C1}, u_{C2}, \ldots, u_{C6}]^T$; the snubber resistance matrix is $\mathbf{R}_{sn} = \mathrm{diag}\{R_{sn1}, R_{sn2}, \ldots, R_{sn6}\}$; the snubber capacitance matrix is $\mathbf{C}_{sn} = \mathrm{diag}\{C_{sn1}, C_{sn2}, \ldots, C_{sn6}\}$; and the currents through the snubber circuits are expressed by the matrix $\mathbf{I}_{sn} = [i_{sn1}, i_{sn2}, \ldots, i_{sn6}]^T$.

In addition, the current matrix is defined as $\mathbf{I}_{d} = [i_{d1}, i_{d2}, \ldots, i_{d6}]^T$, where i_{di} is the sum of corresponding i_{dioi} and i_{sni}. In terms of the above mathematical model of diode, the time domain equation of the rectifier is acquired. Consequently, the current equations of diodes could be written in matrix form as

$$\mathbf{I}_{d} = \mathbf{S}\left[\mathbf{R}_{dio}^{-1}\left(\mathbf{U}_{C} + \mathbf{R}_{sn}\mathbf{I}_{sn} - \mathbf{U}_{d0}\right) + \mathbf{I}_{sn}\right] + (\mathbf{1} - \mathbf{S})\mathbf{I}_{sn} \tag{9}$$

where $\mathbf{S} = \mathrm{diag}\{S_1, S_2, \ldots, S_6\}$, $\mathbf{1}$ is 6×6 unit matrix. The voltage equations of capacitances are expressed in matrix form as

$$\mathbf{I}_{sn} = \mathbf{C}_{sn}\frac{\mathrm{d}}{\mathrm{d}t}\mathbf{U}_{C}. \tag{10}$$

The three-phase currents of AC side satisfy

$$i_a = i_{d1} - i_{d4}, \ \ i_b = i_{d2} - i_{d5}, \ \ i_c = i_{d3} - i_{d6}. \tag{11}$$

The current of DC side i_{dc} is given by

$$i_{dc} = \sum_{i=1}^{3} i_{di} \quad \text{or} \quad i_{dc} = \sum_{i=4}^{6} i_{di}. \tag{12}$$

There are 5 linearly independent equations based on Kirchhoff's voltage law around loops of the circuit composed of 6 diodes

$$
\begin{aligned}
&u_a - (u_{C1} + R_{sn1}i_{sn1}) = u_b - (u_{C2} + R_{sn2}i_{sn2})\\
&u_b - (u_{C2} + R_{sn2}i_{sn2}) = u_c - (u_{C3} + R_{sn3}i_{sn3})\\
&u_a + (u_{C4} + R_{sn4}i_{sn4}) = u_b + (u_{C5} + R_{sn5}i_{sn5})\\
&u_b + (u_{C5} + R_{sn5}i_{sn5}) = u_c + (u_{C6} + R_{sn6}i_{sn6})\\
&u_a - (u_{C1} + R_{sn1}i_{sn1}) - [u_b + (u_{C5} + R_{sn5}i_{sn5})] - u_{dc} = 0
\end{aligned} \tag{13}
$$

Eqs. (9)–(13) are equations for the three-phase bridge rectifier model. Incorporating with the port characteristics of rectifier described by

$$
u_j = u_{0j} - L\frac{\mathrm{d}i_j}{\mathrm{d}t} - R \cdot i_j, \quad j = a, b, c, \tag{14}
$$

and

$$
i_{dc} = C_{dc}\frac{\mathrm{d}u_{dc}}{\mathrm{d}t} + i_{net1}, \tag{15}
$$

all the variables could be calculated.

The equations of different modes of the rectifier are discrepant. Therefore, we should estimate the value of **S** at each discrete time point t_n, $n = 1, 2, 3, \ldots$. For $i = 1, 2, \ldots 6$, and the on/off status of VD_i at t_{n+1} is indicated by S_i^{n+1} which is judged by $U_{\mathrm{dio}i}^n$ calculated at the previous time point t_n:

$$
\begin{aligned}
&\text{If } U_{\mathrm{dio}i}^n \geq U_{\mathrm{d}0i}^n, \text{ then } S_i^{n+1} = 1\\
&\text{If } U_{\mathrm{dio}i}^n < U_{\mathrm{d}0i}^n, \text{ then } S_i^{n+1} = 0
\end{aligned} \tag{16}
$$

Compared with the on/off status S_i^n at t_n, if S_i^{n+1} changed, the initial time step Δt_0 should be modulated. This modulation is due to the fact that the initial discrete time points are not in complete accordance with the actual moment of mode conversion. If the constant time step is kept, the error could cause wrong results.

Supposed that Δt_m is the mth modulated time step of Δt_0, the rules of modulation are stated as following.

Rule 1: For $m = 1$, if S_i does not change, Δt_m remains constant with the value of Δt_0 and $t_{n+1} = t_n + \Delta t_m$. If S_i changes, $\Delta t_m = 0.5 \times \Delta t_0$ and the rule 2 is applied with $m = 2$.

Rule 2: For $m > 1$, the iterative relationships of Δt_m modulation are given as

$$
\begin{cases}
\Delta t_m = \Delta t_{m-1} - 0.5^m\Delta t_0, & \text{if } S_i \text{ changes}\\
\Delta t_m = \Delta t_{m-1} + 0.5^m\Delta t_0, & \text{if } S_i \text{ does not change}
\end{cases} \tag{17}
$$

After m iterations, we can estimate t_{n+1} by the expression $t_{n+1} = t_n + \Delta t_m$. The modulated discrete time points approach to the exact moments of mode conversion of the rectifier very closely.

The input-output model describing the three-phase bridge rectifier is composed of Eq. (9)–Eq. (13), the judgment conditions of on/off status of diode (16), and the rules of time step modulation.

3. CALCULATION OF TRANSMISSION LINE TRANSIENT RESPONSES BY FDTD

According to FDTD, the line current and scattered voltage along the line can be discretized to a set of interlaced current and voltage points both in time and spatial domains. Assume that the two-wire transmission line is divided into NDX sections of length Δx, and the total solution time is divided into segments of length Δt, then the interlaced current and voltage points both in time and spatial domains are denoted by

$$I_k^{n+3/2} = i\left[(k - 1/2)\,\Delta x, (n + 3/2)\,\Delta t\right] \tag{18}$$

$$U_k^{s,n+1} = u^{\text{s}}\left[(k - 1)\,\Delta x, (n + 1)\,\Delta t\right] \tag{19}$$

with $k = 1, 2, \ldots, NDX + 1$, $n = 0, 1, 2, \ldots$. The line current and scattered voltage difference equations given in [16] are

$$\left(\frac{L_0}{\Delta t} + \frac{R_0}{2}\right) I_k^{n+3/2} = \left(\frac{L_0}{\Delta t} - \frac{R_0}{2}\right) I_k^{n+1/2}$$
$$-\frac{1}{\Delta x}\left(U_{k+1}^{s,n+1} - U_k^{s,n+1}\right) + \frac{1}{2}\left(V_{sk}^{n+3/2} + V_{sk}^{n+1/2}\right), \quad k = 1, \ldots, NDX \tag{20}$$

$$\left(\frac{C_0}{\Delta t} + \frac{G_0}{2}\right) U_k^{s,n+1} = \left(\frac{C_0}{\Delta t} - \frac{G_0}{2}\right) U_k^{s,n}$$
$$-\frac{1}{\Delta x}\left(I_k^{n+1/2} - I_{k-1}^{n+1/2}\right) + \frac{1}{2}\left(I_{sk}^{n+1} + I_{sk}^n\right), \quad k = 2, \ldots, NDX. \tag{21}$$

From time domain Agrawal model Eq. (1), we define the corresponding per-unit-length voltage source as

$$V_{sk}(t) = E_{xk}^{\text{inc}}(h, t) - E_{xk}^{\text{inc}}(0, t), \tag{22}$$

and per-unit-length current source as

$$I_{sk}(t) = 0. \tag{23}$$

Next, the terminal conditions are discussed. Because the voltage and current variables in the two lumped parameter networks of the line are at the same position and time, Eqs. (20) and (21) are unsuitable

for the voltage and current variables at each end of the line $u_{\mathrm{net1}}^{\mathrm{s}}$, i_{net1}, $u_{\mathrm{net2}}^{\mathrm{s}}$, i_{net2}. The input-output characteristics of Networks 1 and 2 are expressed by $i_{\mathrm{net1}} = f_1(u_{\mathrm{net1}})$ and $i_{\mathrm{net2}} = f_2(u_{\mathrm{net2}})$, respectively. Supposing that the discrete time points of all variables in the lumped parameter networks are consonant with the scattered voltages, we denote the current variable at each end of the line (I_{net1}^{n+1} and I_{net2}^{n+1}) as

$$I_0^{n+1/2} = \left(I_{\mathrm{net1}}^{n+1} + I_{\mathrm{net1}}^n\right)/2 = \left[f_1\left(U_{\mathrm{net1}}^{n+1}\right) + f_1\left(U_{\mathrm{net1}}^n\right)\right]/2 \quad (24)$$

$$I_{NDX+1}^{n+1/2} = \left(I_{\mathrm{net2}}^{n+1} + I_{\mathrm{net2}}^n\right)/2 = \left[f_2\left(U_{\mathrm{net2}}^{n+1}\right) + f_2\left(U_{\mathrm{net2}}^n\right)\right]/2. \quad (25)$$

For $k = 1$ and $k = NDX + 1$, let $I_{s1} = 0$, $I_{sNDX+1} = 0$, and replace Δx with $\Delta x/2$ in Eq. (21), then substituting Eq. (24) and Eq. (25) into Eq. (21) yields the terminal conditions at the both ends of the line.

$$\left(\frac{C_0}{\Delta t} + \frac{G_0}{2}\right)U_1^{s,n+1} - \left(\frac{C_0}{\Delta t} - \frac{G_0}{2}\right)U_1^{s,n} + \frac{2}{\Delta x}I_1^{n+1/2} - \frac{I_{\mathrm{net1}}^{n+1} + I_{\mathrm{net1}}^n}{\Delta x} = 0 \quad (26)$$

$$\left(\frac{C_0}{\Delta t} + \frac{G_0}{2}\right)U_{NDX+1}^{s,n+1} - \left(\frac{C_0}{\Delta t} - \frac{G_0}{2}\right)U_{NDX+1}^{s,n} - \frac{2}{\Delta x}I_{NDX}^{n+1/2} + \frac{I_{\mathrm{net2}}^{n+1} + I_{\mathrm{net2}}^n}{\Delta x}$$
$$= 0. \quad (27)$$

Combining Eqs. (2), (3) with Eqs. (24), (25) yields the relations of current, scattered voltage and incident voltage at each end of the line. The advantage of this method is that it can be exploited for the line with arbitrary loads, if the characteristics of loads are known.

Taking the case of the system illustrated in Figure 1, the rectifier located at Network 1 and the resistive load located at Network 2 are discussed. Then the corresponding terminal conditions at the source and the load can be written as

$$\left(\frac{C_0}{\Delta t} + \frac{G_0}{2}\right)U_1^{s,n+1} - \left(\frac{C_0}{\Delta t} - \frac{G_0}{2}\right)U_1^{s,n} + \frac{2}{\Delta x}I_1^{n+1/2}$$
$$-\frac{1}{\Delta x R_{net1}}\left[U_{dc}^{n+1} - U_1^{s,n+1} + U_{dc}^n - U_1^{s,n} - \left(U_1^{i,n+1} + U_1^{i,n}\right)\right] = 0 \quad (28)$$

$$\left(\frac{C_0}{\Delta t} + \frac{G_0}{2}\right)U_{NDX+1}^{s,n+1} - \left(\frac{C_0}{\Delta t} - \frac{G_0}{2}\right)U_{NDX+1}^{s,n} - \frac{2}{\Delta x}I_{NDX}^{n+1/2}$$
$$+\frac{1}{\Delta x R_{net2}}\left[U_{NDX+1}^{s,n+1} + U_{NDX+1}^{s,n} + \left(U_{NDX+1}^{i,n+1} + U_{NDX+1}^{i,n}\right)\right] = 0. \quad (29)$$

For the resistive load located at Network 2, the equations of the transmission line by FDTD are composed of Eqs. (20), (21) and Eqs. (28), (29) with respect to the interconnection between the lumped parameter networks and the transmission line. To ensure the stability

of recursion relations, the initial time step Δt_0 and spatial step Δx should satisfy the Courant condition $\Delta t_0 \leq \Delta x/v$, where v is the phase velocity of propagation of the wave. Then the modified time step $\Delta t_m < \Delta t_0$ in the three-phase bridge rectifier model can also satisfy this condition.

The method could be utilized to calculate the transient responses of each junction of the system and any position along the transmission line effectively.

4. EXPERIMENTAL VERIFICATION

In order to validate the mathematical model and algorithm presented in this paper, a lightning surge simulated experiment of the AC/DC power system is conducted. The experiment circuit is illustrated in Figure 1 without inductances and filtering capacitance. The experimental parameters show as below: the three-phase sinusoidal alternating source voltages are balanced; the virtual value is $U_R = 10\,\mathrm{V}$; and frequency is $f = 50\,\mathrm{Hz}$. The critical voltage of each diode is $0.7\,\mathrm{V}$; the resistance of each diode is $0.01\,\Omega$; and the resistance load is $R_{\mathrm{net2}} = 200\,\Omega$. For the two-wire transmission line, the length of line is $l = 1\,\mathrm{m}$, and the per-unit-length parameters of the line are

$$R_0 = 1.268 \times 10^{-3}\,\Omega/\mathrm{m}, \quad L_0 = 2.328 \times 10^{-6}\,\mathrm{H/m},$$
$$G_0 = 0\,\mathrm{S/m}, \qquad\qquad C_0 = 4.77 \times 10^{-12}\,\mathrm{F/m}.$$

The EMC PARTNER Transient-2000 generates the voltage pulse to simulate the lightning pulse, which is used to interfere with the steady running system. The waveform of voltage pulse is shown in Figure 2, and the peak voltage is $134\,\mathrm{V}$.

$U_{\mathrm{EMP}}(t)$ is the value of voltage pulse at arbitrary moment. The EMP is added to the (k_m)th segment in the form of distributed voltage
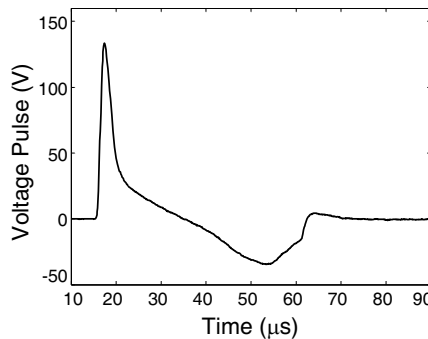
Figure 2. The waveform of voltage pulse.

source. Therefore, substitute $-U_{\text{EMP}}^{n+1}$ for $\Delta x(V_{sk}^{n+3/2} + V_{sk}^{n+1/2})/2$ if $k = k_m$, and the distributed voltage source is $V_{sk} = 0$ if $k \neq k_m$ in the line current difference equation Eq. (20). In addition, the lumped voltage sources at the ends of the line are $u_1^i = u_{NDX+1}^i = 0$ for each discrete time point. Substituting these into Eqs. (20), (21) and Eqs. (28), (29), and combining with the difference equations of lumped parameter network, the transient responses of system with EMP interference are calculated. Figure 3 compares the calculation results with the experiment ones for (a) voltage responses at $x = l$ and (b) voltage at $x = 0$. The waveforms show a good agreement between the calculation and experiment results.
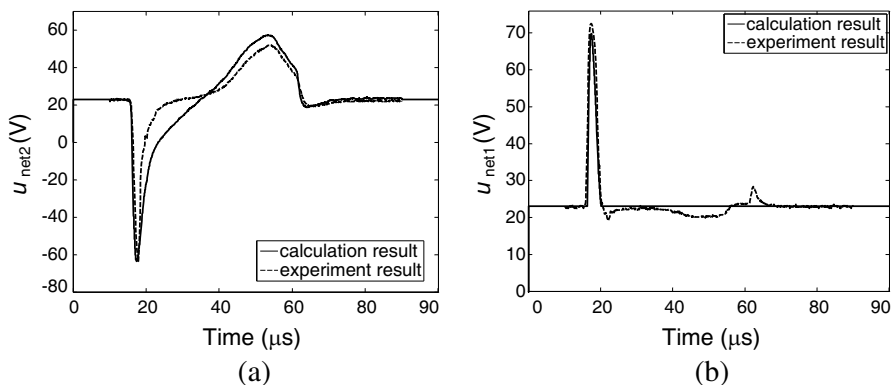
Figure 3. Comparison of calculation and experiment results: (a) voltage responses at $x = l$; (b) voltage responses at $x = 0$.

5. NUMERICAL EXAMPLES

The transient responses of the AC/DC power system with the incident plane wave interference, shown in Figure 1, are calculated by the above method. The following primary circuit parameters have been chosen for this analysis: the parameters of the balanced three-phase AC voltage are $U_R = 120\,\text{V}$, $f = 400\,\text{Hz}$. The critical voltage of each diode is $0.8\,\text{V}$; the resistance of each diode is $0.01\,\Omega$; the snubber circuits are all resistive snubber; and each snubber resistance is $300\,\Omega$. The inductance of AC side is $L = 6 \times 10^{-5}\,\text{H}$, and filtering capacitance of DC side is $C_{\text{dc}} = 2 \times 10^{-3}\,\text{F}$. The load located at Network 2 is assumed to be completely resistive with value $R_{\text{net2}} = 10\,\Omega$. The length of the transmission line is $l = 5\,\text{m}$, and the separation is $d = 0.1\,\text{m}$. The

per-unit-length parameters are

$$R_0 = 524 \times 10^{-3}\,\Omega/\text{m}, \quad L_0 = 309 \times 10^{-9}\,\text{H/m},$$
$$G_0 = 905 \times 10^{-9}\,\text{S/m}, \quad C_0 = 144 \times 10^{-12}\,\text{F/m}.$$

The incident E-field is described by

$$E(t) = E_0 \left(\mathrm{e}^{-\beta t} - \mathrm{e}^{-\alpha t} \right) \tag{30}$$

where the peak value is $5 \times 10^3\,\text{V/m}$, $\alpha = 1 \times 10^9\,\text{s}^{-1}$, and $\beta = 5 \times 10^8\,\text{s}^{-1}$. Figure 4 plots the E-field waveform for these parameters. After discretizing them in time domain and substituting into the field-to-line coupling difference equations, the transient responses can be calculated.
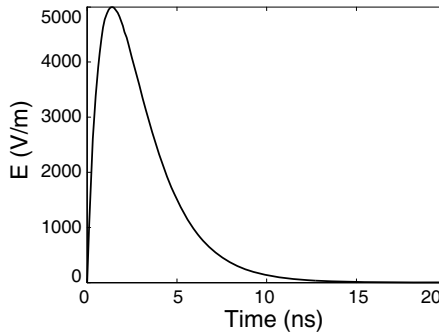
Figure 4. The waveform of E-field pulse signal.

5.1. Linear Resistance and AC/DC Circuit at Network 1

If the power system runs steadily without any inference, the ratio of the voltage u_{net1} to the current i_{net1} approaches a constant with the LC filter circuit in this example. Consequently, a constant K_{net1} is set $K_{\text{net1}} = u_{\text{net1}}/i_{\text{net1}} = 12.62$. To illustrate the differences between the responses for the linear and nonlinear loads, firstly we assume that Network 1 is a linear load with a resistance of $12.62\,\Omega$, and the EMP interferes with the system at a certain time. In this case, the transient responses are calculated. Then we also calculate the transient responses when Network 1 is an AC/DC power electronic circuit with EMP interference.

Figure 5 plots the transient responses at $x = l$ in the case of Network 1 of the line with an AC/DC circuit and with a linear resistive load with EMP interference. The calculation results illustrate that in the case of an AC/DC circuit located at Network 1, there is an increase

in the amplitudes of both the voltage u_{net2} across R_{net2} and the current i_{net2} through R_{net2}, and the attenuation of the pulse becomes slower compared with the case of a resistance located at Network 2. Thus, there is more instantaneous power delivered to R_{net2} under the EMP interference when Network 1 of line is a three-phase bridge rectifier.
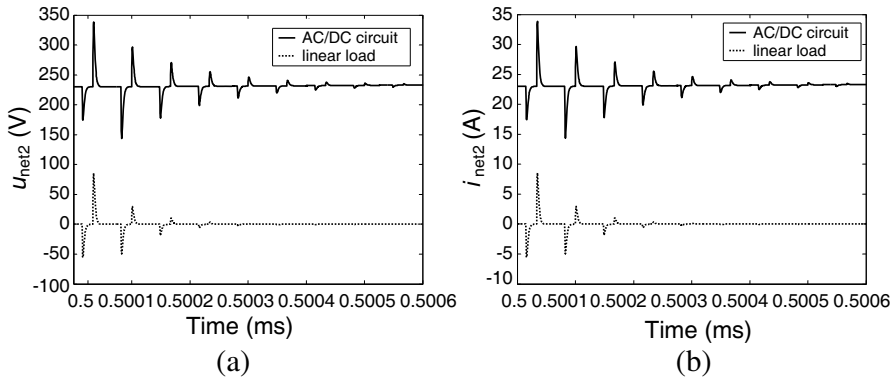
Figure 5. Comparison of the responses at $x = l$ in the case of Network 1 of the line with an AC/DC circuit and with a linear load: (a) voltage responses, (b) current responses.

5.2. Different Resistive Loads at Network 2

In the case of the AC/DC circuit located at Network 1, the length of the transmission line is 5 m, and the transient responses at $x = l$ with the different resistances $R_{net2} = 1\,\Omega$, $R_{net2} = 10\,\Omega$ and $R_{net2} = 100\,\Omega$ are plotted in Figure 6.

The dashed lines in Figure 6 represent the transient load voltage and current with $10\,\Omega$ which were presented previously in Figure 5. The solid lines and dash dot lines in Figure 6 demonstrate the corresponding transient responses when R_{net2} is $1\,\Omega$ and $100\,\Omega$, respectively. As can be seen in Figure 6, with the increasing value of the resistance, the amplitude attenuation of EMP response is getting faster. Furthermore, with the effect of EMP on the voltage u_{net2} increasing, the effect of EMP on the current i_{net2} decreases correspondingly.

5.3. Different Lengths of the Line

In the case of the AC/DC circuit located at Network 1 and the resistance $R_{net2} = 10\,\Omega$ located at Network 2, Figure 7 illustrates the comparison of the voltage responses of Network 2 with the length of the transmission line $l = 1$ m, $l = 5$ m, and $l = 10$ m, respectively. As
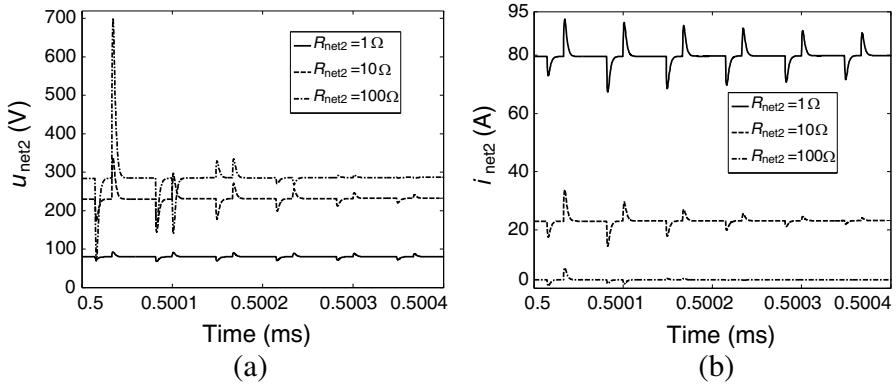
Figure 6. Comparison of the responses at $x = l$ with the different resistances: (a) voltage responses, (b) current responses.
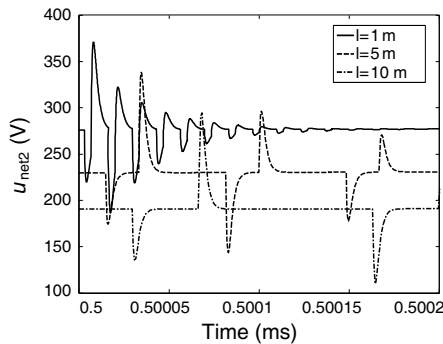
Figure 7. Comparison of the voltage responses at $x = l$ with the different lengths of the transmission line.

revealed by Figure 7, the attenuation of EMP responses shows slow trends as the length raised. The current responses of Network 2 are similar, which are not plotted here.

6. CONCLUSION

A new method for analysis of transient electromagnetic performance of AC/DC power system with EMP interference has been derived. The major works of modeling and validation include:

1) The method integrated the analysis method of the electric circuits and electromagnetic fields to study the coupled field-circuit

problems has been utilized for the AC/DC power systems in this paper, which could also be further extended to the independent electrical power systems containing DC/DC converter, inverter, etc.

2) We have proposed an input-output model of three-phase bridge rectifier which can avoid the complex conditions of mode conversion and make the programming easier due to the uniform expressions without judgement of modes. Moreover, a rule of modulating the time step has been presented in order to approach to the exact moments of mode conversion of the rectifier very closely.

3) For validation, the experiment has been designed, and the calculation and experiment results show a good agreement to validate the method.

ACKNOWLEDGMENT

REFERENCES

1. Taylor, C., R. Satterwhite, and C. Harrison, "The response of a terminated two-wire transmission line excited by a nonuniform electromagnetic field," *IEEE Trans. Antennas Propag.*, Vol. 13, No. 6, 987–989, 1965.

2. Agrawal, A. K. and H. J. Price, "Transient response of multiconductor transmission lines excited by a nonuniform electromagnetic field," *IEEE Trans. Electromagn. Compat.*, Vol. 22, No. 2, 119–129, 1980.

3. Rachidi, F., "Formulation of the field-to-transmission line coupling equations in terms of magnetic excitation field," *IEEE Trans. Electromagn. Compat.*, Vol. 35, No. 3, 404–407, 1993.

4. Wang, Z.-Z., Y.-W. Li, B.-X. Lu, F. Zhang, and B. Yi, "Study on numerical method of transient electromagnetic field coupling to secondary cable in substations," *Proceedings of the CSEE*, Vol. 28, No. 3, 107–111, 2008 (in Chinese).

5. Ren, H.-M., B.-H. Zhou, T.-B. Yu, and Z. Wang, "Coupling effects of LEMP on aerial multiconductor power lines," *High Pow. Las. Particle Beams*, Vol. 17, No. 10, 1539–1543, 2005 (in Chinese).

6. Xie, H., J. Wang, R. Fan, and Y. Liu, "Study of loss effect of transmission lines and validity of a SPICE model

in electromagnetic topology," *Progress In Electromagnetics Research*, Vol. 90, 89–103, 2009.

7. Zhang, H., J.-H. Wang, and W.-Y. Liang, "Study on the applicability of extracted distributed circuit parameters of non-uniform transmission lines by equivalent circuit method," *Journal of Electromagnetic Waves and Applications*, Vol. 22, No. 5–6, 839–848, 2008.

8. Tesche, F. M., M. V. Ianoz, and T. Karlsson, *EMC Analysis Methods and Computational Models*, John Wiley & Sons, New York, 1996.

9. Huang, C.-C., "Analysis of multiconductor transmission lines with nonlinear terminations in frequency domain," *Journal of Electromagnetic Waves and Applications*, Vol. 19, No. 8, 1069–1083, 2005.

10. Tesche, F. M., "On the analysis of a transmission line with nonlinear terminations using the time-dependent BLT equation," *IEEE Trans. Electromagn. Compat.*, Vol. 49, No. 2, 427–433, 2007.

11. Xie, L. and Y.-Z. Lei, "Transient response of a multiconductor transmission line with nonlinear terminations excited by an electric dipole," *IEEE Trans. Electromagn. Compat.*, Vol. 51, No. 3, 805–810, 2009.

12. Xie, H., J. Wang, D. Sun, R. Fan, and Y. Liu, "Spice simulation and experimental study of transmission lines with TVSs excited by EMP," *Journal of Electromagnetic Waves and Applications*, Vol. 24, No. 2–3, 401–411, 2010.

13. Martinez, J. A. and F. Castro-Aranda, "Lightning performance analysis of overhead transmission lines using EMTP," *IEEE Trans. Pow. Deliv.*, Vol. 20, No. 3, 2200–2210, 2005.

14. Rahimian, M. S., S. H. H. Sadeghi, and R. Moini, "LEMP coupling with medium voltage overhead lines and its effects on low voltage networks with power electronic devices," *3rd International Symposium on Electromagnetic Compatibility*, 115–118, Beijing, 2002.

15. Dommel, H. W., *EMTP Theory Book*, China WaterPower Press, Beijing, 1991.

16. Paul, C. R., *Analysis of Multiconductor Transmission Line*, John Wiley & Sons, New York, 1994.